Materials and Structures (2022) 55:158
https://doi.org/10.1617/s11527-022-01993-x

ORIGINAL ARTICLE

Modelling microalgae biofouling on porous buildings materials: a novel approach

Enrico Quagliarini · Benedetta Gregorini · Marco D'Orazio

Received: 17 March 2021 / Accepted: 8 June 2022 / Published online: 1 July 2022

Abstract A correct assessment of microalgae growth on porous building materials (i.e.: fired bricks, sandstones and limestones) can provide a useful tool for researchers and practitioners. In fact, it may help predicting the biofouling damage extension and it can assist the experts in a correct planning of maintenance interventions to limit costs. The literature regarding such issue outlined the Avrami's model as the most recurrent one, even considering the influence of biocidal treatments on the substrate. However, it seems to have some limitations when the growth is very fast or, conversely, when the latency time is extended over the time. Therefore, a different modelling approach is here proposed, by using the logistic function (extensively used i.e. in population growth). Results reveal that the logistic function seems to succeed in better modelling the available experimental data. Moreover, it seems to overcome the limits of the Avrami's model, as well as to be less influenced by the main drivers of microalgae growth, such as porosity and roughness of the substrate, biocides treatments and environmental conditions (temperature).

Keywords Microalgae growth · Façades biodeterioration · Avrami's model · Logistic function · Porous building materials

List of symbols

$X(t)$	Covered area by algae biofouling (–)
A_c/A_t	Final covered area ratio parameter (–)
r	Intrinsic growth rate parameter (day^{-1})
t_p	Growth inflection point parameter (day)
n	Avrami's exponent for time variation (–)
$R_{\%}$	R Factor index (%)
exp_1, …, exp_3	The experimental measures of the 3 samples respectively (–)
exp_m	The average experimental value (–)
$exp_{m,i}$	The average experimental value for the ith time (–)
m_{tot}	The total slope of the average experimental data (–)
m_i	The ith slope of the average experimental data (–)

1 Introduction

The biodeterioration caused by microorganisms is one of the first causes of deterioration of construction

E. Quagliarini (✉) · B. Gregorini · M. D'Orazio
Department of Construction, Civil Engineering and Architecture (DICEA), Università Politecnica Delle Marche, via Brecce Bianche, 60131 Ancona, Italy
e-mail: e.quagliarini@univpm.it

B. Gregorini
e-mail: b.gregorini@pm.univpm.it

M. D'Orazio
e-mail: m.dorazio@univpm.it

materials and it usually leads to a decrease in their performances [1, 2]. The main actors that cause degradation can be identified in fungi, mould, cyanobacteria and green microalgae [3, 4]: they produce chemical and mechanical degradation of the surfaces themselves, and subsequently, acting as first colonizers, they form a conducive substrate to more complex biological forms (e.g. mosses and lichens) [5]. In addition, their high adaptability to external conditions let the biodeterioration phenomena to spread on several construction materials, being them porous (such as concrete, brick, stones [6, 7]) and non-porous ones (i.e. ETICS [8]), when subject to different environmental conditions (e. g. temperature, humidity, light, condensation [9, 10]). Starting from discoloration, biodeterioration may end up causing high maintenance and repair costs for the external surfaces of constructions, monuments, outdoor furniture and so on, even leading to hazards to human health (e.g. slipping problems when it occurs on pathways) [9, 11, 12]. Among these microorganisms, microalgae growth is one of the less investigated phenomena to the authors' knowledge, especially compared to mould and fungi. Moreover, recent literature focused in describing its influencing factors (e.g. substrata properties, environmental conditions and effects of biocides treatments) but it is quite poor on growth modelling and failure model side [13–17].

From an engineering point of view, a correct modeling of the microalgae biofouling phenomenon can provide a useful tool both for predicting the damage on the various porous building materials and for the correct planning of maintenance interventions so as to be able to limit their costs [16, 18].

Currently, the most widespread model applied to porous building materials is the Avrami's model. It was firstly provided by Tran [17] dealing with cement mortars where microalgae growth reached the complete covering of the tested samples. Subsequent changes to the initial formulation (modified Avrami's model) allowed the successfully application of the model to other porous building materials, where the microalgae could not reach the total coverage of the tested samples [14, 16], i.e. slightly porous and slightly rough fired bricks surfaces [14, 15], materials treated with biocides [14–16] and when the environmental conditions limited their development (e.g. low temperature) [13].

However, two important limitations of such model can be pointed out. A previous work [15] highlighted that one of the Avrami's flaws occurs when the growth rate is very fast (i.e.: on materials having high porosity and/or high roughness) and the latency phase is missing. Due to the analytical formulation and the constraints adopted [15] to ensure the physical aspects, the curve has a minimum value equal to 0 and a latency phase that prevents the curve to develop as fast as the experimental microalgae biofouling. The second limitation, conversely, occurs when the latency time extends over the growth time, e.g. for materials with low porosity and/or roughness. According to the first derivative, such model is used to analytically show a decreasing trend between time zero and the latency time. As a consequence, the predicted biofouling coverage in this interval could be rather poor.

To overcome such issue, Tran [17] proposed to consider null the coverage before the latency time. Anyway, if we want a model where only before the inoculation/storage of algae, that is, at time $t = 0$, as for the experimental set-up we are going to deal with in this paper, it can be considered null, and then it is a not decreasing function, the Avrami's model does not succeed in.

An alternative approach could be thus preferred to overcome those limitations.

The use of the logistic function could be a valid help in this direction. Besides its historical wide use when dealing with population growth models [19–21], it was, in fact, quite employed i.e. in the biofuel industry for what concerns biological description of microalgae growth [22]. Besides, numerous studies adopted this formulation to simulate the experimental data of in vitro microalgae cultivations [23–28]. Concerning the description of biofouling on porous building materials, the logistic formula has been recently successfully applied only in one study on mold growth [29], but no application about microalgae growth is known up to now to the authors' knowledge.

Hence, the aim of this work is to apply the logistic model for describing microalgae growth on some of the most recurrent porous building materials (fired bricks, limestones and sandstones), previously analyzed through the Avrami's model. Moreover, since microalgae growth curves are strongly influenced by substrate properties, (i.e. porosity and roughness), environmental conditions (i.e. temperature) and eventual surface treatments, such factors are also considered for the models' accuracy. By comparing the results, this work wants to verify if the first one:

– can better overlap experimental data and overcome the previous cited limits than the second one;
– is less influenced by the main factors influencing the microalgae growth, such as porosity and roughness of the substrate, environmental temperature, as well as biocides treatments.

2 Materials and methods

2.1 Theory

A brief description of the Avrami's model we refer to is reported in Appendix 3.

Instead, the logistic function adopted in this work is defined by Eq. (1), proposed in [24, 29]:

$$X(t) = \frac{A_c}{A_t} \cdot \left(\frac{1}{1 + \exp^{-r(t-t_p)}} \right) \quad (1)$$

where, microalgae coverage X (–) is a function of time t (day) and the three parameters, namely A_c/A_t, r and t_p, can be defined from experimental measures. In particular, the first one is the maximum covered area ratio (–), being A_c the area covered by microalgae and A_t the total area of the sample. It represents the horizontal asymptote ranging between 0 and 1. The r parameter (day^{-1}) can be defined as the intrinsic growth rate [24] while the t_p parameter (day) is defined as the inflection point of the growth curve and it is the day in which microalgae coverage $(A_c/A_t)/2$ is reached. In this work both r and t_p are calculated through iterations by minimizing the least squares value between experimental data and calculated values [24]. In particular, according to such method, the two parameters were calculated through iteration as a pair of values (t_p, r) that minimizes the sum of the squares of the residuals. Residuals were considered as the differences between the experimental values $X_{exp_{m,i}}$ and the ones obtained with the logistic equation $X(t_p, r)_i$ for each measuring time [30], as reported in Eq. 1a.

$$(t_p, r) : \min \left(\sum_{t=i} \left(X_{exp_{m,i}} - X(t_p, r)_i \right)^2 \right) \quad (1a)$$

Moreover, the model first derivative is always higher than 0 for every time values: hence, no decreasing trend can be observed as happening for the Avrami's equation (see Sect. 3.2).

It is important to underline that in the following sections Eq. 1 is compared to equation C1:

– from time $t = 0$ to the time of the last experimental measure (condition 1);
– by considering the coverage equal to zero before the latency time, for taking into account the physical aspects involved in its formulation [17] (condition 2).

2.2 Experimental tested materials

Previous experimental microalgae growth data, already modelled by the (modified) Avrami's model, on fired bricks, sandstones and limestones [13–16] are selected, as reported in Table 1. The relative Avrami's curves are thus collected from such references, while the logistic ones are determined from the beginning for all the materials (Table 1).

2.3 Methods for the comparison

2.3.1 Overlapping the experimental data

The first comparison involves the assessment of which model could better overlap the experimental data. To assess that, the comparison is run generally evaluating: how many times the models overlap the data and their fitting quality. Concerning the values out per each model, this work evaluates when they are out according to each growth phase and how far from the experimental data they are.

For the first comparison, this works determines the percentage of values that validates condition (2):

$$\min(X_{exp_1}, \ldots, X_{exp_3})_i \leq X(t = i) \leq \max(X_{exp_1}, \ldots, X_{exp_3})_i \quad (2)$$

where $X(t = i)$ is the calculated covered area for both the models at the ith time, that is, the time (days) when the measure was made during the microalgae growth (e.g.: 0, 7 days, 14 days, …, 70 days) and X_{exp1}, …, X_{exp3} correspond to the experimental measures of the 3 samples respectively.

To the same aim, a comparison between the fitting quality index $R_{\%}$ (–) of the two models is run. This index was previously adopted for the Avrami's law [13, 14, 16, 17], and it is calculated according to (3):

Table 1 List of the porous building materials considering substrate properties, temperature and surface treatments [13–16]

Substrate properties					Temperature		Surface treatment			
Typology	Refs	Name	Porosity (–)	Roughness (μm)	T = 10 °C	T = 27.5 °C	None	TiO_2	TiO_2 + Ag	TiO_2 + Cu
Brick	[14]	LSU	0.19	2.4		✔	✔			
		LST	0.19	2.4		✔		✔		
		LRU	0.19	2.8		✔	✔			
		LRT	0.19	2.8		✔		✔		
	[15]	NNt	0.19	2.8		✔	✔			
		NAg	0.19	2.8		✔			✔	
		NCu	0.19	2.8		✔				✔
	[13]	AS	0.19	4.5	✔		✔			
		AS	0.19	4.5		✔	✔			
		AR	0.19	5.54	✔		✔			
		AR	0.19	5.54		✔	✔			
		B	0.25	2.95	✔		✔			
		B	0.25	2.95		✔	✔			
	[14]	HSU	0.37	1.1		✔	✔			
		HST	0.37	1.1		✔		✔		
		HRU	0.37	8.9		✔	✔			
		HRT	0.37	8.9		✔		✔		
	[15]	ANt	0.37	8.9		✔	✔			
		AAg	0.37	8.9		✔			✔	
		ACu	0.37	8.9		✔				✔
	[13]	CS	0.44	6.6	✔		✔			
		CS	0.44	6.6		✔	✔			
		CR	0.44	7.6	✔		✔			
		CR	0.44	7.6		✔	✔			
Sandstone	[16]	A2	0.05	7.9		✔	✔			
		A2T	0.05	7.9		✔		✔		
		A1	0.08	7.6		✔	✔			
		A1T	0.08	7.6		✔		✔		
Limestone	[16]	C3	0.08	2		✔	✔			
		C3T	0.08	2		✔		✔		
		C1	0.09	2.6		✔	✔			
		C1T	0.09	2.6		✔		✔		
		C2	0.18	2.6		✔	✔			
		C2T	0.18	2.6		✔		✔		

$$R_{\%} = \sqrt{\frac{\sum_{t=i}\left(X(t=i) - X_{\exp_{m,i}}\right)^2}{\sum_{t=i} X_{\exp_{m,i}}}} \cdot 100 \qquad (3)$$

where $X(t = i)$ and $X_{\exp_{m,i}}$ represent the calculated and the average experimental data at time $t = i$, respectively. This value expresses the deviation between experimental data and simulated one, that is, the more it tends to zero the more the analytical model overlaps the measured data.

For the second step, the percentage of the values resulting out of the experimental range is run according to (4):

$$\left(\frac{\text{number of } X_{\text{out}}}{\text{number of } X_{\text{tot}}}\right)_{G_p} \tag{4}$$

comparing the number of times values are out (X_{out}) to the number of total values (X_{tot}) resulting in each specific growth phase G_p (i.e. latency, exponential and stagnation).

To avoid subjective interpretations, the discretization of the average experimental data into the three phases is run according these steps:

1. the total slope of the experimental data m_{tot} was determined as the linear incremental ratio between the starting point (0;0) and the ending point (t_{end}; X_{max}) from the experimental data, where t_{end} corresponds to the last measuring time.
2. the ith slope m_i is determined between the covered area at time i and the previous measure at time $i - 1$;
3. the three phases are evaluated according to condition (5)

$$\begin{cases} \text{Exponential} & m_i > m_{\text{tot}} \\ \text{Latency, Stagnation} & m_i \leq m_{\text{tot}} \end{cases} \tag{5}$$

This discretization method defines the exponential phase as the phase in which the growth slope m_i is higher than the overall linear growth (m_{tot}). Conversely, both the latency and stagnation take place when m_i is equal or lower than m_{tot}, respectively, right before and after the exponential phase. Figure 1 shows an example of such discretization: the first 11 experimental data and the last 9 values are grouped respectively in the latency/stagnation phase, since their m_i values are always lower than m_{tot}; conversely, the remaining experimental values can be grouped in the exponential phase because their m_i are higher than the m_{tot}. In this way, it is possible to define a latency phase where the coverage is not a constant equal to zero, but it has an incremental ratio, even if small.

The goal of the last comparison is to evaluate eventual trend of under/over estimation for such out values and, thus, to asses if one of the models is closer to the experimental data, even when not properly overlapping the data. For every ith out values, the underestimation/overestimation is calculated by determining the difference between the calculated $X(t = i)$ and the minimum/maximum experimental value among the three sample $(X_{\text{exp}_1}, \ldots, X_{\text{exp}_3})_i$ according to (6):

$$\begin{cases} \dfrac{X(t=i) - \min(X_{\text{exp}_1}, \ldots, X_{\text{exp}_3})_i}{A_c/A_t}, & \text{if } X(t=i) < \\ \min(X_{\text{exp}_1}, \ldots, X_{\text{exp}_3})_i \\ \dfrac{X(t=i) - \max(X_{\text{exp}_1}, \ldots, X_{\text{exp}_3})_i}{A_c/A_t}, & \text{if } X(t=i) > \\ \max(X_{\text{exp}_1}, \ldots, X_{\text{exp}_3})_i \end{cases} \tag{6}$$

Moreover, a normalization of such differences to the total covered area A_c/A_t is set in order to have comparable results. In fact, the total covered area significantly differs among all the materials, ranging between 0.10 and 1.00 [13–16]. Condition (6) is determined for both the models. Boxplot analysis is run to describe the trend and distribution of such values for each phase.

2.3.2 *Overcoming the Avrami's flaws*

The first step of this section wants to validate the hypothesis that the Avrami's model is not able to correctly simulate microalgae growth for ANt, ACu and AAg materials because the latency phase is missing [15]. In order to verify that, the discretization above is applied to such materials by verifying the presence/absence of the latency phase. Subsequently, by determining the logistic curves for such materials, the work verifies whether the logistic model is able to overcome this flaw. A graphical test is also adopted to check the overcoming of the second Avrami's flaw for all the materials with the latency time higher than 0, for both conditions 1 and 2 reported in Sect. 2.1.

2.3.3 *Correlation with the influencing factors*

The third comparison is run to assess which model is lesser influenced by the microalgae influencing factors such as porosity and roughness, surface treatments, as well as different environmental conditions (temperature). To evaluate the correlation with each factor alone, three subsets are formed:

1. Porosity and Roughness subset: with all the untreated material under T = 27.5 °C;
2. Temperature subset: all the untreated material under T = 10 °C and T = 27.5 °C, respectively;

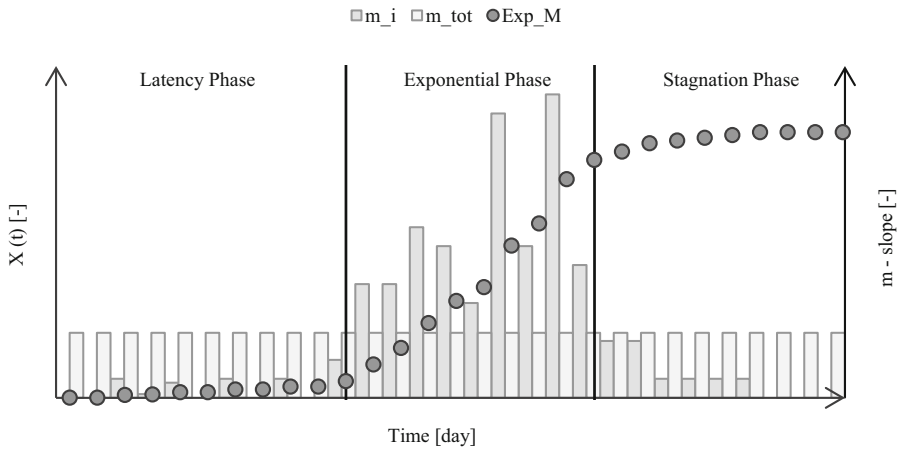

Fig. 1 Example of average experimental data discretization into the latency/exponential/ stagnation phase. Black dots represent the average experimental data; vertical bars represent the *m* values, respectively grey for the *i*th value and white for the total. The 2nd axis refers to the *m* values

3. Surface Treatment subset: all the treated and respectively untreated materials under $T = 27.5$ °C.

Three categories are correlated to each subset. The first one is the numbers of values inside the experimental range, the second one involves the fitting quality index $R_{\%}$ (–) and the third one considers the values out according to each growth phase (latency, exponential and stagnation phase).

In particular, the effect of porosity and roughness is considered as a combined effect through a fitting surface determined as a 1st degree polynomial equation fitted by using MATLAB R2017b software [31]. A linear regression is considered for temperature and surface treatments. Since this last one is a binary regressor (untreated/ treated), binary indicator variables are used respectively 0 for the untreated materials and 1 for the treated ones [32]. The coefficient of determination R^2 (–) is used to assess if a correlation between each model and the cited above influencing factors is present ($R^2 \geq 0.50$) [32] and the relative trends are then evaluated through scatter plot, only in affirmative cases.

3 Results

3.1 Overlapping the experimental data

It is worth underlining right off that there are no significant differences by considering the comparison between the logistic model and the Avrami's one declined on both the two conditions reported in Sect. 2.1, thus, what is reported in the following can be considered valid in either case.

The only exception is for the check on values out and growth phases. This particular case will be specified hereafter.

Figure 2 shows the percentage of the values of the Avrami's and logistic model that falls within the minimum and maximum values of the experimental data. For fired brick (Fig. 2a), about the 2/3 of the Avrami's values fall within the given experimental range. For the logistic model, these values raise up to about 3/4. For the stony materials (Fig. 2b) 70% of values are included in the experimental range for both the models. In addition, limestones and sandstone, singularly taken, have comparable result.

Figure 3 shows the scatter plots that compare the $R_{\%}$ obtained for both the models applied to fired bricks and stones. For fired bricks (Fig. 3a), it is evident that the logistic model presents better results: the $R_{\%}$ values are all below the bisector line of the graph. In particular, when the Avrami's model is less correct with $R_{\%}$ values ranging between 45 and 60% (2 treated bricks and 1 untreated), the logistic model is able to increase the accuracy down to 10%. For stones (Fig. 3b), both models are, instead, really precise since all the $R_{\%}$ values are below 1%.

When analyzing the values out for each single phase (Fig. 4a), the first evidence is that the two models miss about 1 experimental value out of 2 in the latency phase for both bricks and stones. A little bit better behavior is reached only for bricks when considering the Avrami's model with no algal coverage from time zero to latency time (42% of values out instead of 44% of Fig. 4a).

The accuracy of the two models in lying inside the experimental ranges increases in the other two phases.

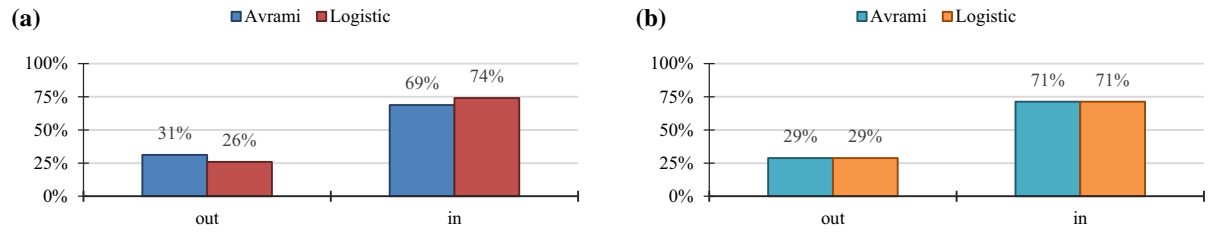

Fig. 2 Analysis of Avrami's and logistic values within the experimental range for: **a** bricks; **b** stones

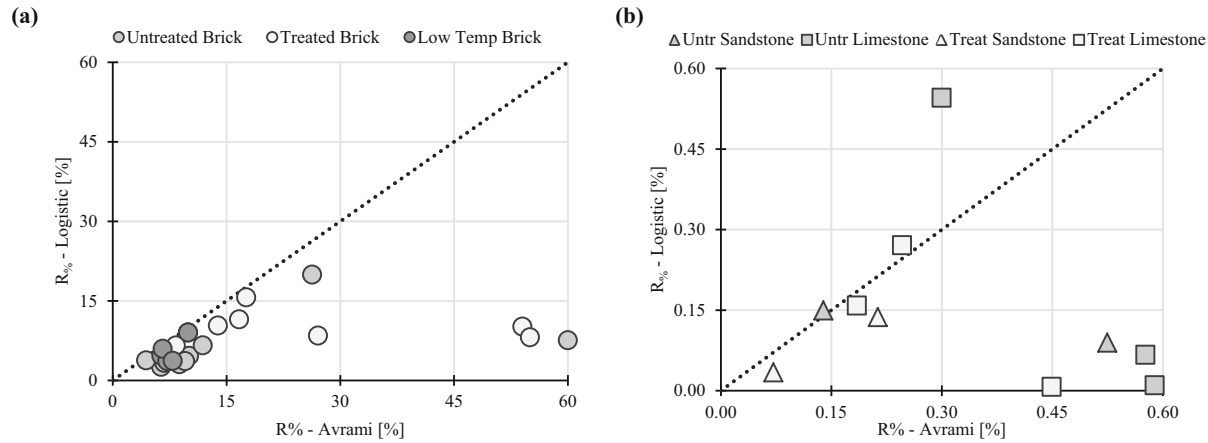

Fig. 3 Comparative scatter plot between the Avrami's and the logistic function $R_{\%}$ parameter: **a** fired bricks; **b** sandstone and limestone. Dotted line represents the graph bisector line

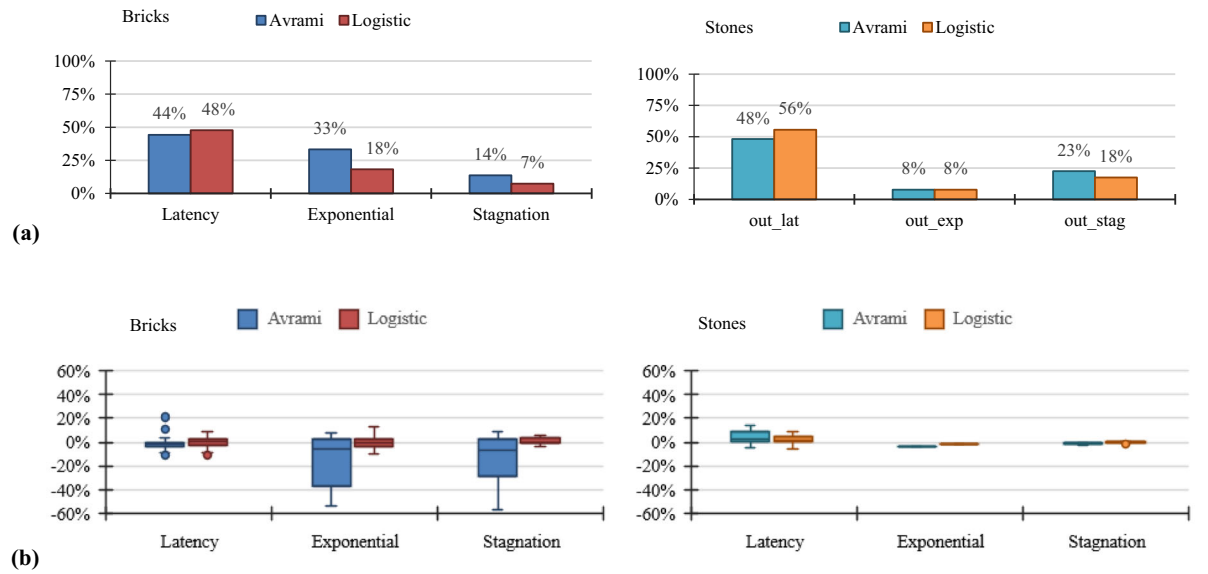

Fig. 4 Analysis of Avrami's and logistic values out for bricks and stones: **a** trend correlation between values out and growth phases; **b** boxplot analysis for under/overestimation trends

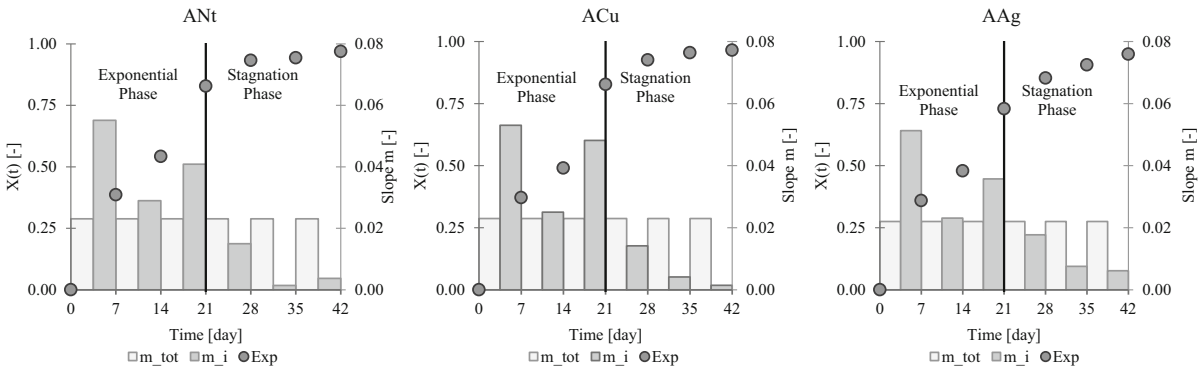

Fig. 5 Data discretization into the latency/exponential/stagnation phase for material ANt, ACu and AAg. Black dots represent the average experimental data; vertical bars represent the *m* values, respectively white for the total and grey for the *i*th value. The 2nd axis refers to the *m* values

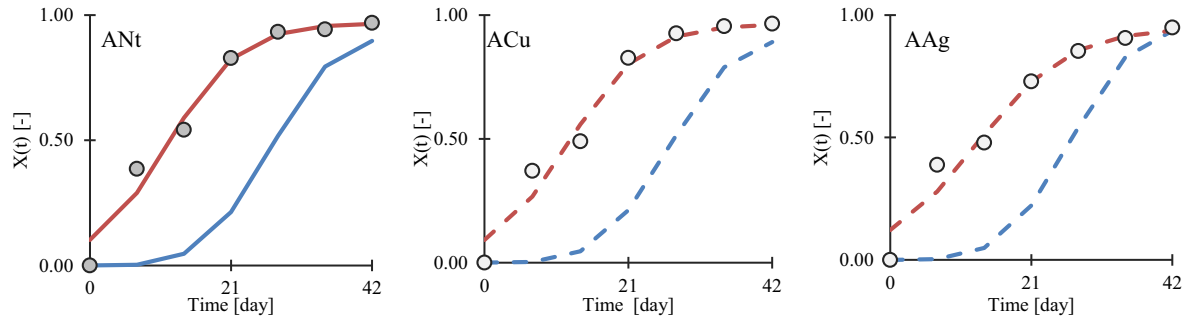

Fig. 6 Fast algae growth. Points indicate the average experimental data under optimal growth conditions on bricks without (grey) and with surface treatments (white); the blue curve indicates the Avrami's model; the red curve indicates the Logistic Function model (dashed lines indicate bricks with surface treatments)

In particular, the logistic model halves the Avrami's percentages for fired bricks, while comparable results hold for stones, for both limestone and sandstone. Lastly, Fig. 4b shows how far the analytical values are from the experimental ones. In fact, the logistic model reduces the overestimation and underestimation of the experimental data, especially in the exponential and stagnation phases of bricks.

3.2 Overcoming Avrami's flaws

Figure 5 confirms what previously hypothesized and reported in literature [15]: the trend of microalgae growth on materials ANt, ACu and AAg escapes the latency phase. As shown in Fig. 5, the m_i slope are higher than the total slope m_{tot} from the growth start until 21 days, denoting the starting trend as exponential.

For such materials, the logistic model better simulates the fast growth, escaping the latency phase, than the Avrami's one, that it is not able at all to predict most of the experimental points, as shown in Fig. 6. It is obvious that, in this case, the values obtained at time zero are not null and it could have no physical meaning, except you can consider that as due to the (rapid) effect of the inoculation over the samples. Anyway, this could be a gap to be filled for future research. At this moment, it is better to have a (logistic) model that can predict better most of the experimental points (all of the experimental points rather than one, in this case), especially during the exponential and the stagnation phase, for practical purposes.

The logistic model is also able to overcome the second Avrami's flaw, when this model is declined by condition 1 in Sect. 2.1, thanks to the differences in its formulation. In fact, its equation shows an increasing first derivative for every time value. Nevertheless, Fig. 7 shows one of the most significative scenarios

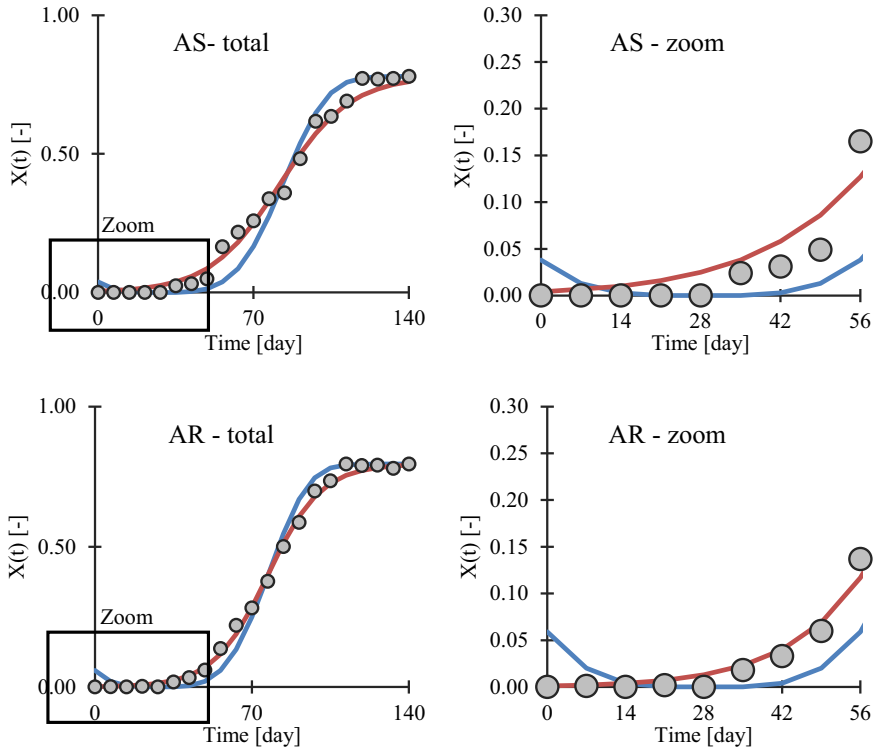

Fig. 7 Comparison between average experimental data, Avrami's model curve and Logistic for materials AS-AR with slow growth [13]. Points indicate the average experimental data under optimal growth conditions (grey); blue line indicates the Avrami's model; red line indicates the Logistic

representing such problem and the simulating differences between the two models. Such scenario refers to materials AS and AR, with very low porosity and/or roughness (see Table 1). Since the latency time was set to 27 days [13], a particularly extended latency time, the Avrami's model has a slight decreasing trend with a starting point at about + 0.05, while the logistic does not.

For sake of clarity, since the curves of the other bricks and stony materials (listed in Table 1) showed barely visible differences are not here reported, but they can be found in Appendix 1.

3.3 Correlation with microalgae growth influencing factors

The first result of the correlation analysis is that the accuracy of both models for bricks is poorly affected by microalgae growth influencing factors (Fig. 8) since all the obtained R^2 values are lower than 0.50. However, when comparing the two models, we can note that the logistic one is more performing in respect to substrate properties and temperature. In fact, for such categories, 8 logistic R^2 values out of 10 are lower than the respective Avrami's one. For surface treatments, the correlation is barely null for both of them. The only $R^2 \geq 0.50$ is the one between the values out during the exponential phase and the temperature for the Avrami's model.

"Lat", "Exp" and "Stag" indicate respectively the latency, exponential and stagnation phase.

For what concerns the stony materials, a strong correlation between the porosity and roughness of the substrate and the model accuracy can be observed (Fig. 9). In particular, the most of R^2 values are higher than 0.50 for the values inside and outside, whereas the ones referring to the logistic model are still lower than the Avrami's one. As for bricks, surface treatments have no influence on both the models' accuracy.

"Lat", "Exp" and "Stag" indicate respectively the latency, exponential and stagnation phase.

Figures 10 and 11 show all the scatter plots for $R^2 \geq 0.50$. According to that, it is possible to note that: for bricks (Fig. 10), Avrami's model has fewer values out for low temperature values; for stones, the lower the porosity is, the more correct both the models are. When $R^2 \leq 0.50$, e.g. the $R^2 = 0.17$ for logistic values out in the latency phase (Fig. 11), datapoint are quite scattered, thus their determined trend are not predictive.

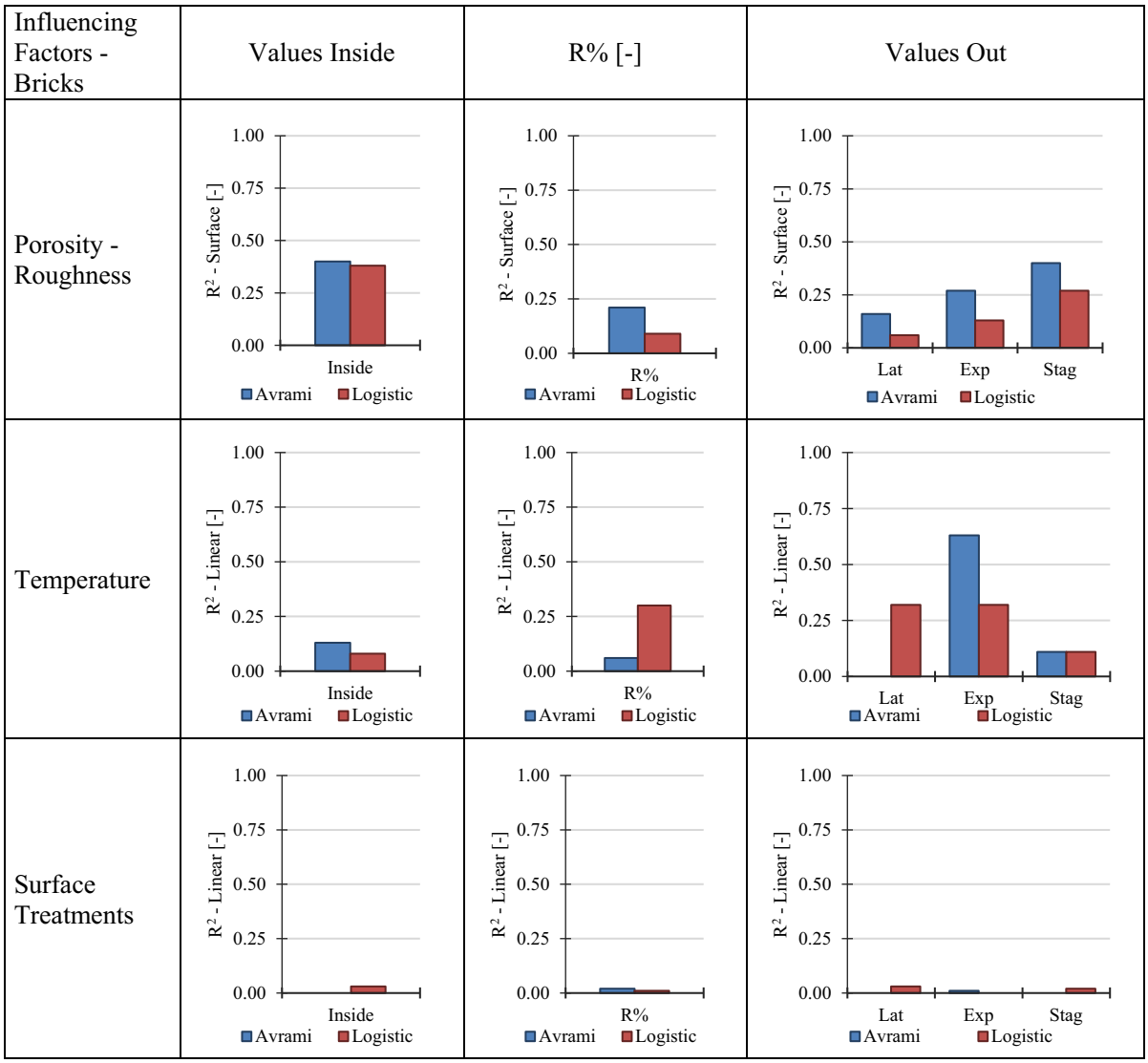

Fig. 8 Correlation analysis (R^2) between the two model and the microalgae influencing factors for fired bricks

Nevertheless, all the remaining trend, with $R^2 < 0.50$ for bricks and stones, are reported in Appendix 2.

4 Conclusion

Predictive models for microalgae growth on porous building materials can provide a useful tool for engineers and practitioners to support correct and adequate maintenance actions, thus limiting intervention costs, as well as to understand the powerful of protective or conservative treatments. In this work, a novel approach, using the logistic function, never applied for microalgae growth on porous building materials up to now, is proposed and compared to the most recurrent one in literature: the Avrami's model. The comparison was made by using the same experimental dataset available in literature. The results showed that the logistic model seems to be more reliable than the Avrami's model. In fact, it is: (1) accurate as the Avrami's model, or even more accurate when applied to bricks, in overlapping the experimental data, by reducing the over/underestimations and increasing the fitting quality; (2) able to overcome the Avrami's flaws both when the growth is too fast or too slow; (3) lesser or even not at all disturbed by the

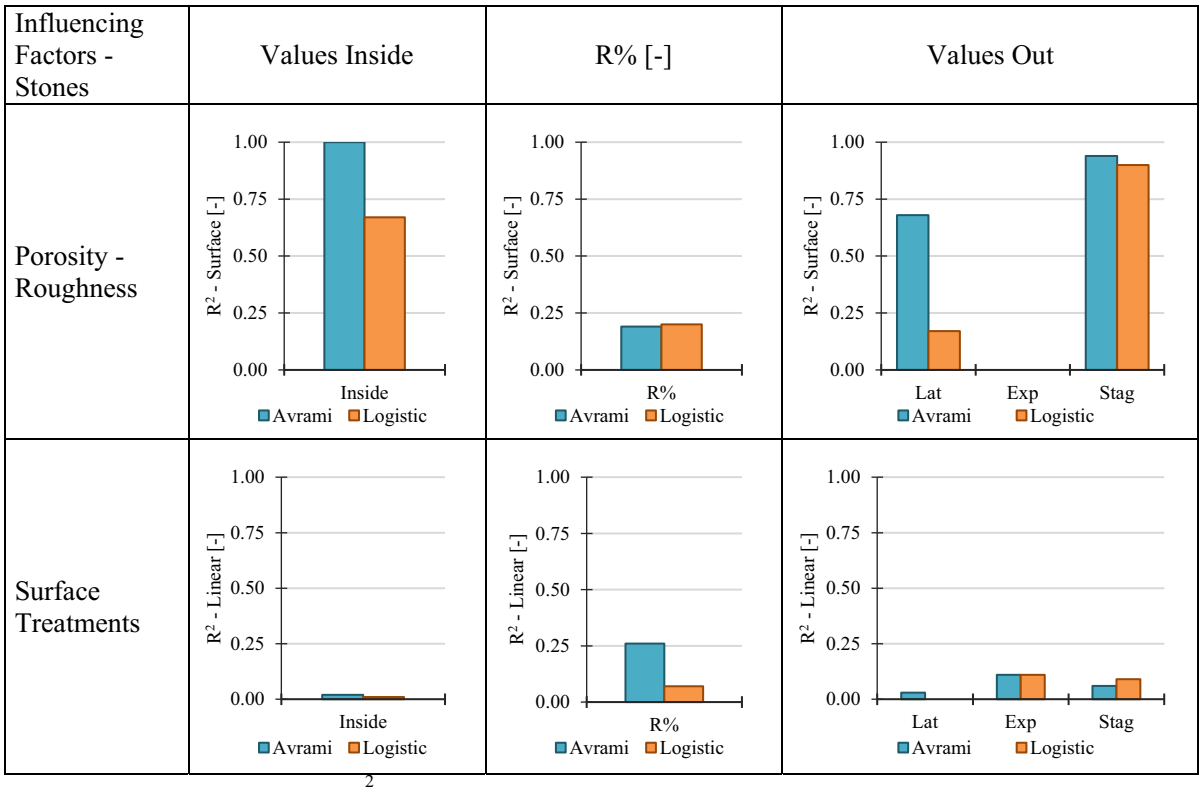

Fig. 9 Correlation analysis (R^2) between the two model and the microalgae influencing factors for stones

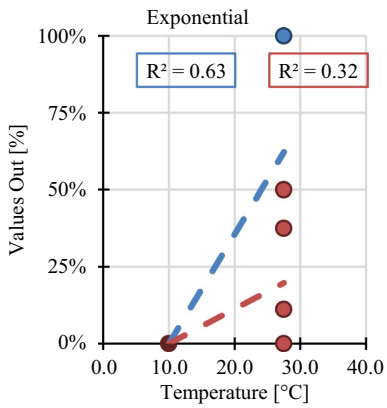

Fig. 10 Trend analysis for bricks: scatter plot for $R^2 \geq 0.50$. Brick values out in exponential phase. Points indicate the determined values, the dashed blue and red lines indicate, respectively, the fitting results for the Avrami's and the Logistic model

influencing factors for microalgae growth. It is worth pointing out that the logistic model used in this study is a pure mathematic model with no correlations with the physic of the studied phenomenon. On the other side, in the considered Avrami's one, physical aspects of the phenomenon are taken into account. This leads necessarily to constraints on its parameters and then lower correlation between the experimental data and the fit.

Nevertheless, future works should deepen the influence of the substrate properties on the models' accuracy, especially the stony ones since the materials subset was limited compared to the brick one, as soon as other experimental data will be available. Besides, the logistic model should be tested on other materials (e.g. wood, plaster, mortars and ETICS, as well as, carbonated cementitious ones) composing monuments, buildings and furniture than can be prone to microalgae biofouling. Future research should be also oriented towards the use of it for characterizing the overall material bio-receptivity. Finally, a possible development of the work may concern the implementation of a real failure model which, starting from the characteristics of the substrate, considering different environmental conditions (mainly temperature) and

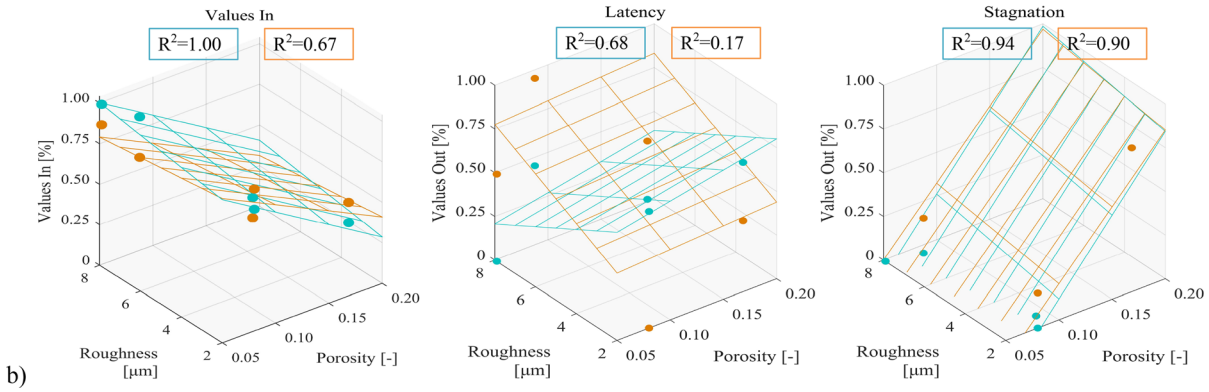

Fig. 11 Trend analysis: scatter plot for $R^2 \geq 0.50$. Stone values in, latency values out and stagnation values out. Points indicate the determined values, the light blue and light red meshes indicate, respectively, the fitting results for the Avrami's and the Logistic model

exploiting the logistic equation, will be able to describe the phenomenon of biofouling over time.

Author contributions The paper reflects the authors' own research and analysis in a truthful and complete manner. The paper properly credits the meaningful contributions of co-authors. In fact, all authors have been personally and actively involved. Consent to submit has been received explicitly from all co-authors.

Funding Open access funding provided by Università Politecnica delle Marche within the CRUI-CARE Agreement. This research has received funding from the Università Politecnica delle Marche under the grant agreement "Ph.D. Program in Civil, Environmental and Building Engineering and Architecture", financing the author Benedetta Gregorini (resolution of the Rectoral Decree n. 1034 – 18/10/2017).

Data availability All materials and sources are properly disclosed, and proper references are inserted.

Code availability Not applicable.

Declarations

Conflict of interest The authors have no conflicts of interest to declare that are relevant to the content of this article.

Fig. 12 Comparison between average experimental data, Avrami's model curve and Logistic Function curve for fired bricks [13–15], listed according to Table 1. Points indicate the average experimental data under optimal growth conditions (grey), under low temperature (dark grey) and treated (white); blue line indicates the Avrami's model; red line indicates the Logistic Function curve; dotted and dashed lines relatively indicate materials under low temperature and with surface treatments ▶

Appendix 1

Figure 12 reports all the logistic curves determined and applied to the literature experimental data and compared to the Avrami's curve for fired bricks materials [13–15]. Materials are listed according to Table 1

Figure 13 shows the logistic curve determined and applied to the stony experimental data compared to the respective Avrami's curve [16]. Materials are listed according to Table 1.

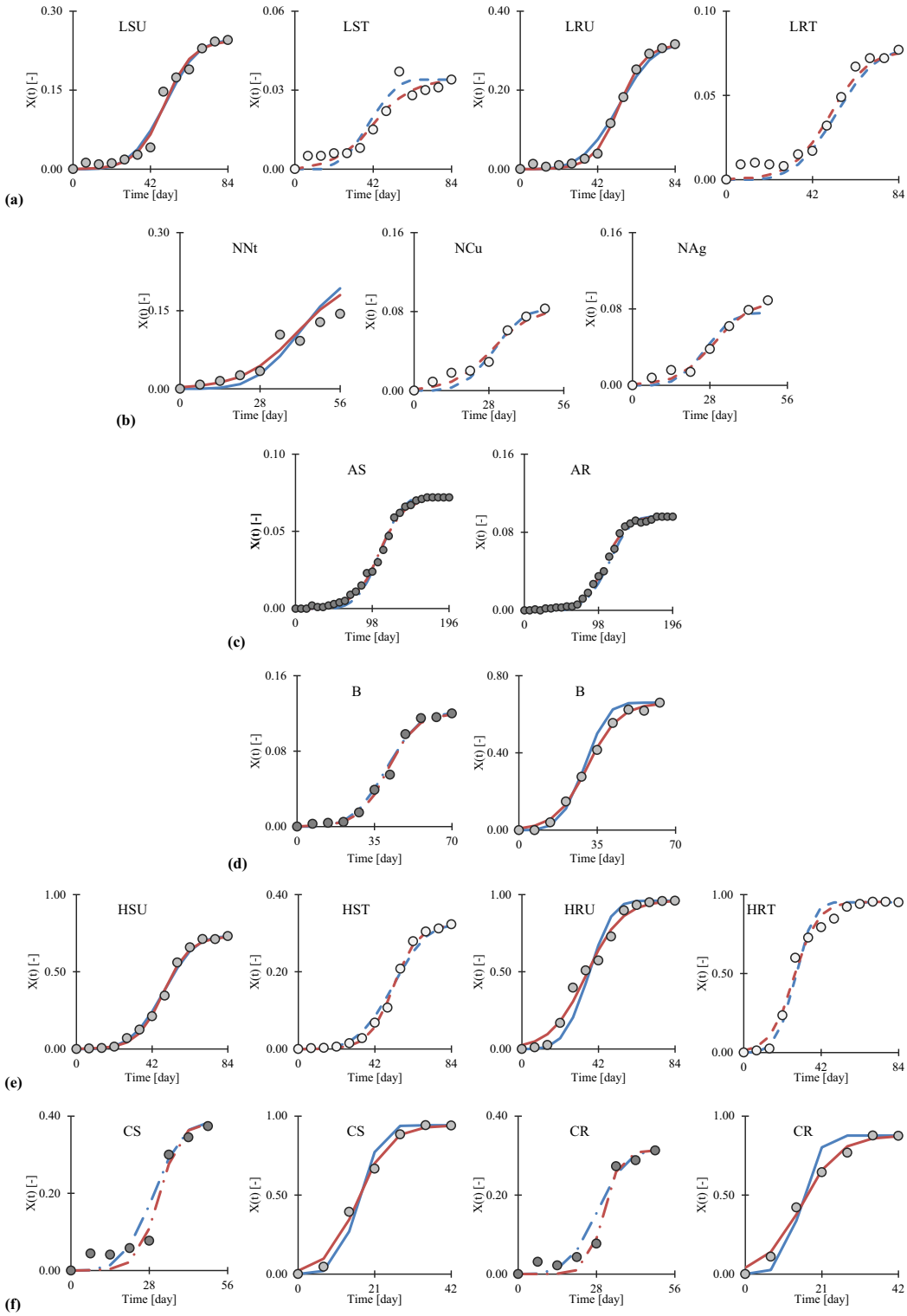
(a)
LSU
LST
LRU
LRT
(b)
NNt
NCu
NAg
(c)
AS
AR
(d)
B
B
(e)
HSU
HST
HRU
HRT
(f)
CS
CS
CR
CR
X(t) [-]
Time [day]

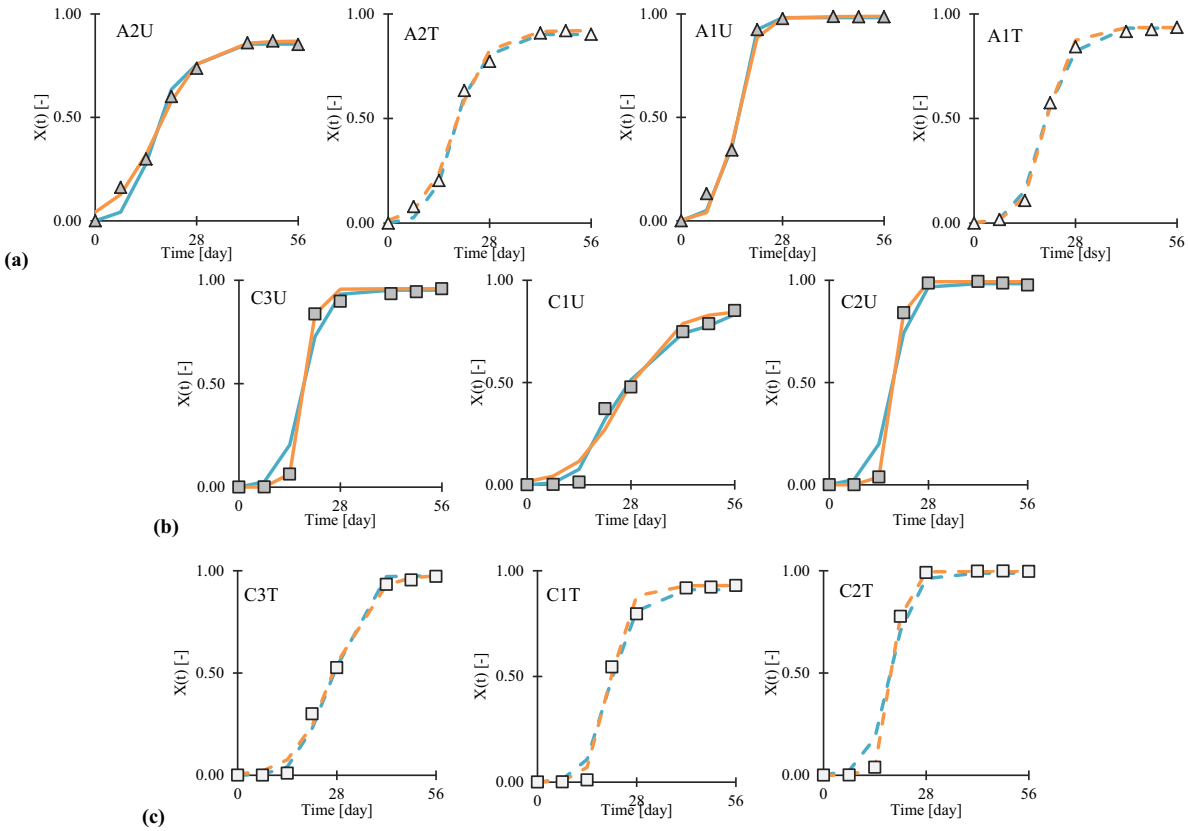

Fig. 13 Comparison between average experimental data, Avrami's model curve and Logistic Function curve for stones [16]: **a** sandstone (triangle); **b**, **c** limestone (square). Points indicate the average experimental data under optimal growth conditions (grey) and treated (white); light blue line indicates the Avrami's model light red line indicates the Logistic Function curve; dashed lines relatively indicate materials with surface treatments

Appendix 2

Figure 14 shows all the scatter plot and the determined trend for all the $R^2 \leq 0.50$ for the brick surfaces, indicating also their respective R^2.

Points indicate the determined values, lines indicate the fitting results, respectively blue for Avrami's model and red for the logistic.

Figure 15 shows all the scatter plot and the determined trend for all the $R^2 \leq 0.50$ for the stony materials, indicating also their respective R^2.

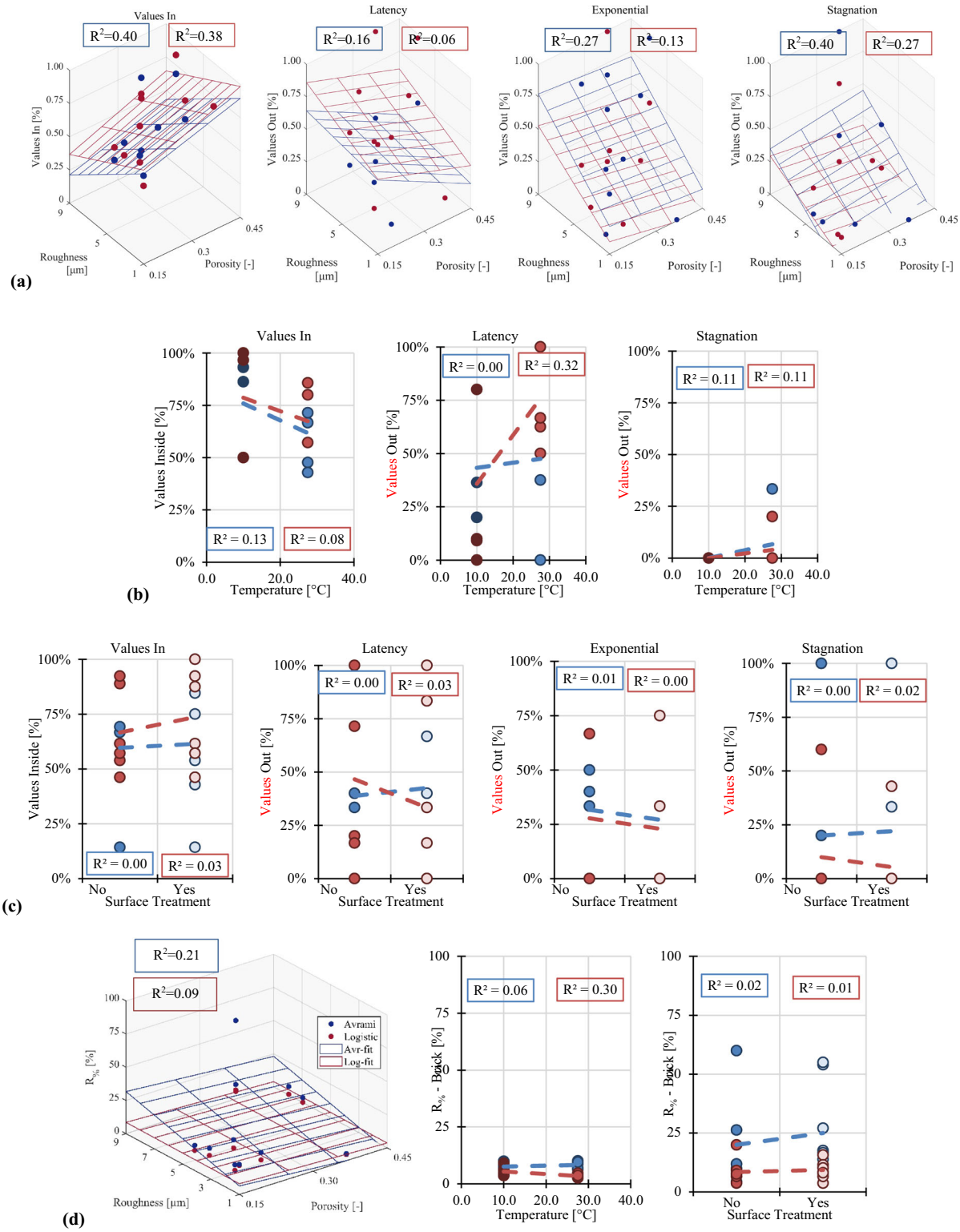

Fig. 14 Correlation analysis for bricks: **a** Values in and out with Porosity and Roughness, **b** Values in and out with Temperature; **c** Values in and out with Surface treatment; **d** $R_{\%}$ with all the three influencing factors

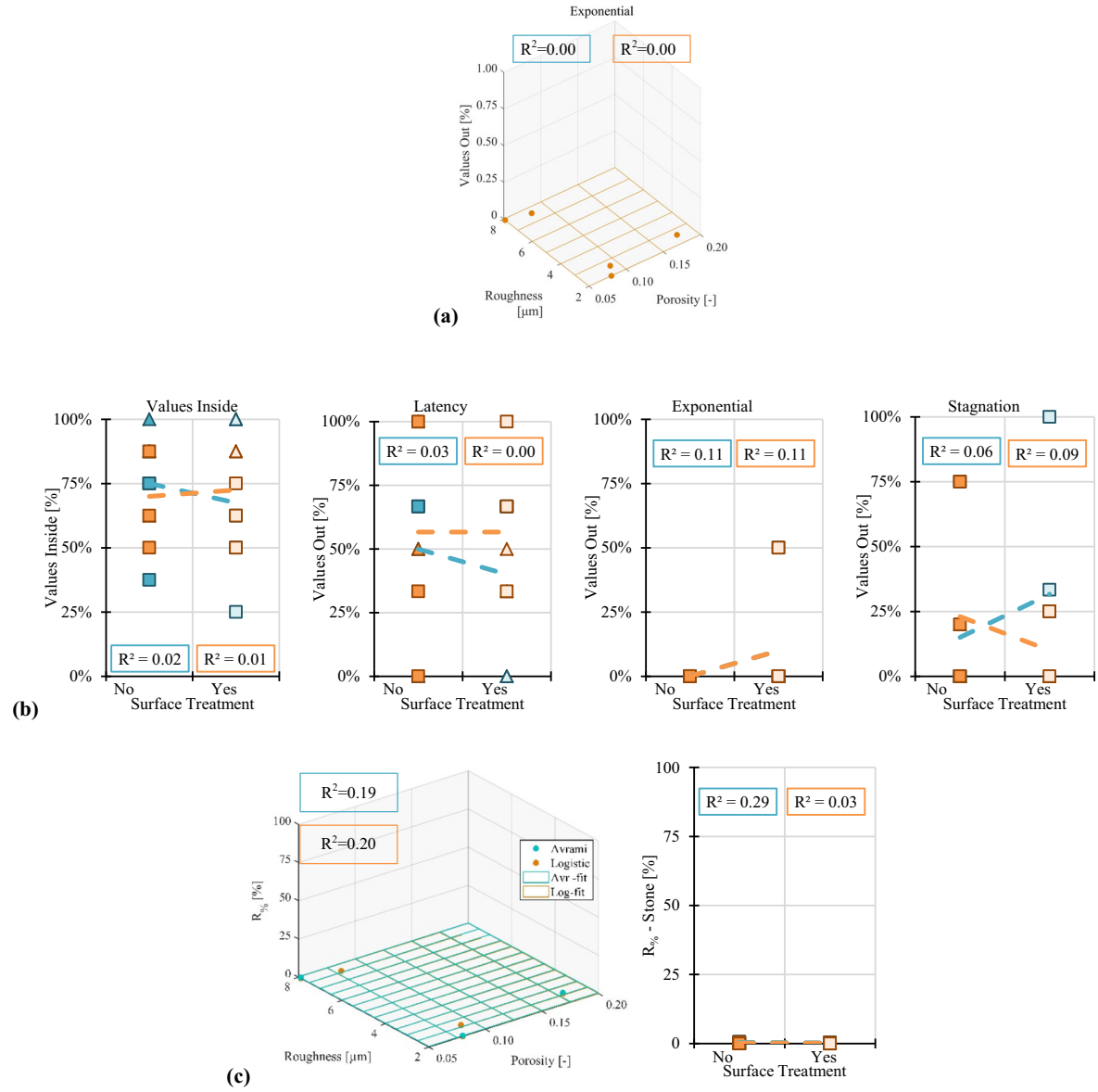

Fig. 15 Correlation analysis for stones: **a** Values in and out with Porosity and Roughness, **b** Values in and out with Surface treatment; **c** $R_{\%}$ with all the three influencing factors. Points indicate the determined values, lines indicate the fitting results, respectively light blue for Avrami's model and light red for the logistic

Appendix 3

The Avrami's model we refer to is based on nucleation and the subsequent growth of nuclei [17], this means that given a material in phase A (uncolonized material), the nucleation corresponds to the formation of nuclei of phase B (colonized material), while the growth corresponds to the increase in the size of these nuclei after their first appearance. A simple equation can summarize this process, as reported in Eq. 8 [14, 16].

$$X(t) = (1 - \exp^{-K(t-t_1)^n}) \cdot \frac{A_c}{A_t} \quad (8)$$

where $X(t)$ (–) is the percentage of covered surface area by algae, t_1 (day) is the latency time, K (–) is a constant depending on the material, n can be assumed equal to 4 [14], A_c is the covered area by algae at the end of the accelerated growth test, and A_t is the total area of the sample.

References

1. Gaylarde C, Ribas Silva M, Warscheid T (2003) Microbial impact on building materials: an overview. Mater Struct 36:342–352. https://doi.org/10.1007/BF02480875
2. Warscheid T, Braams J (2000) Biodeterioration of stone: a review. Int Biodeterior Biodegrad 46:343–368. https://doi.org/10.1016/S0964-8305(00)00109-8
3. Gaylarde CC, Gaylarde PM (2005) A comparative study of the major microbial biomass of biofilms on exteriors of buildings in Europe and Latin America. Int Biodeterior Biodegrad 55:131–139. https://doi.org/10.1016/j.ibiod.2004.10.001
4. Ferrari C, Santunione G, Libbra A et al (2015) Review on the influence of biological deterioration on the surface properties of building materials: organisms, materials, and methods. Int J Des Nat Ecodyn 10:21–39. https://doi.org/10.2495/DNE-V10-N1-21-39
5. Barberousse H, Lombardo RJ, Tell G, Couté A (2006) Factors involved in the colonisation of building façades by algae and cyanobacteria in France. Biofouling 22:69–77. https://doi.org/10.1080/08927010600564712
6. Barberousse H, Ruot B, Yéprémian C, Boulon G (2007) An assessment of façade coatings against colonisation by aerial algae and cyanobacteria. Build Environ 42:2555–2561. https://doi.org/10.1016/j.buildenv.2006.07.031
7. Giovannacci D, Leclaire C, Horgnies M et al (2013) Algal colonization kinetics on roofing and façade tiles: Influence of physical parameters. Constr Build Mater 48:670–676. https://doi.org/10.1016/j.conbuildmat.2013.07.034
8. D'Orazio M, Cursio G, Graziani L et al (2014) Effects of water absorption and surface roughness on the bioreceptivity of ETICS compared to clay bricks. Build Environ 77:20–28. https://doi.org/10.1016/j.buildenv.2014.03.018
9. Miller AZ, Sanmartín P, Pereira-Pardo L et al (2012) Bioreceptivity of building stones: a review. Sci Total Environ 426:1–12. https://doi.org/10.1016/j.scitotenv.2012.03.026
10. Flores-Colen I, de Brito J, de Freitas VP (2008) Stains in facades' rendering—diagnosis and maintenance techniques' classification. Constr Build Mater 22:211–221. https://doi.org/10.1016/j.conbuildmat.2006.08.023
11. Coutinho ML, Miller AZ, Macedo MF (2015) Biological colonization and biodeterioration of architectural ceramic materials: an overview. J Cult Herit 16:759–777. https://doi.org/10.1016/j.culher.2015.01.006
12. Borderie F, Tête N, Cailhol D et al (2014) Factors driving epilithic algal colonization in show caves and new insights into combating biofilm development with UV-C treatments. Sci Total Environ 484:43–52. https://doi.org/10.1016/j.scitotenv.2014.03.043
13. Quagliarini E, Gianangeli A, D'Orazio M et al (2019) Effect of temperature and relative humidity on algae biofouling on different fired brick surfaces. Constr Build Mater 199:396–405. https://doi.org/10.1016/J.CONBUILDMAT.2018.12.023
14. Graziani L, Quagliarini E, D'Orazio M (2016) TiO2-treated different fired brick surfaces for biofouling prevention: experimental and modelling results. Ceram Int 42:4002–4010. https://doi.org/10.1016/j.ceramint.2015.11.069
15. Graziani L, Quagliarini E, D'Orazio M (2016) The role of roughness and porosity on the self-cleaning and anti-biofouling efficiency of TiO2-Cu and TiO2-Ag nanocoatings applied on fired bricks. Constr Build Mater 129:116–124. https://doi.org/10.1016/j.conbuildmat.2016.10.111
16. Graziani L, Quagliarini E (2018) On the modelling of algal biofouling growth on nano-TiO2 coated and uncoated limestones and sandstones. Coatings 8:54. https://doi.org/10.3390/coatings8020054
17. Tran TH, Govin A, Guyonnet R et al (2013) Avrami's law based kinetic modeling of colonization of mortar surface by alga Klebsormidium flaccidum. Int Biodeterior Biodegrad 79:73–80. https://doi.org/10.1016/j.ibiod.2012.12.012
18. Caneva G, Nugari MP, Salvadori O (1991) Biology in the conservation of works of art. ICCROM
19. Tashiro T, Yoshimura F (2019) A neo-logistic model for the growth of bacteria. Physica A 525:199–215. https://doi.org/10.1016/J.PHYSA.2019.03.049
20. Jin W, McCue SW, Simpson MJ (2018) Extended logistic growth model for heterogeneous populations. J Theor Biol 445:51–61. https://doi.org/10.1016/J.JTBI.2018.02.027
21. Verhulst PF (1845) Recherches mathématiques sur la loi d'accroissement de la population. Nouv mémoires l'Académie R des Sci B-lett Bruxelles 18:14–54
22. Lee E, Jalalizadeh M, Zhang Q (2015) Growth kinetic models for microalgae cultivation: a review. Algal Res 12:497–512. https://doi.org/10.1016/J.ALGAL.2015.10.004
23. Banks HT, Collins E, Flores K et al (2017) Statistical error model comparison for logistic growth of green algae (*Raphidocelis subcapitata*). Appl Math Lett 64:213–222. https://doi.org/10.1016/J.AML.2016.09.006
24. Kong W, Huang S, Shi F et al (2018) Study on Microcystis aeruginosa growth in incubator experiments by combination of Logistic and Monod functions. Algal Res 35:602–612. https://doi.org/10.1016/J.ALGAL.2018.10.005
25. Xin L, Hong-ying H, Ke G, Ying-xue S (2010) Effects of different nitrogen and phosphorus concentrations on the growth, nutrient uptake, and lipid accumulation of a freshwater microalga *Scenedesmus* sp. Bioresour Technol 101:5494–5500. https://doi.org/10.1016/j.biortech.2010.02.016
26. Khalseh R (2016) Evaluation of different kinetics for bioethanol production with emphasis to analytical solution of substrate equation. Theor Found Chem Eng 50:392–397. https://doi.org/10.1134/S0040579516040357

27. Surendhiran D, Vijay M, Sivaprakash B, Sirajunnisa A (2015) Kinetic modeling of microalgal growth and lipid synthesis for biodiesel production. 3 Biotech 5:663–669. https://doi.org/10.1007/s13205-014-0264-3
28. Stemkovski M, Baraldi R, Flores KB, Banks HT (2016) Validation of a mathematical model for green algae (*Raphidocelis subcapitata*) growth and implications for a coupled dynamical system with Daphnia magna. Appl Sci. https://doi.org/10.3390/app6050155
29. Berger J, Le Meur H, Dutykh D et al (2018) Analysis and improvement of the VTT mold growth model: application to bamboo fiberboard. Build Environ 138:262–274. https://doi.org/10.1016/j.buildenv.2018.03.031
30. Tobergte DR, Curtis S (2013) Applied statistics using SSPS, Statistica, Matlab and R. J Chem Inf Model. https://doi.org/10.1017/CBO9781107415324.004
31. MathWorks (2017) Curve Fitting Toolbox - User 's Guide - Matlab R2017b
32. Stock JH, Watson MW (2015) Introduction to econometrics, 3rd edn. Pearson, Chicago